Journal of Oceanography, Vol. 63, pp. 711 to 720, 2007

Short Contribution

Estimating the Geostrophic Velocity Obtained by HF Radar Observations in the Upstream Area of the Kuroshio

RYOKO TOKESHI[1], KAORU ICHIKAWA[2,3]*, SATOSHI FUJII[4,5], KENJI SATO[4] and SHOICHIRO KOJIMA[4]

[1]*Interdisciplinary Graduate School of Engineering Sciences, Kyushu University, Kasuga-Koen, Kasuga, Fukuoka 816-8580, Japan*
[2]*Research Institute for Applied Mechanics, Kyushu University, Kasuga-Koen, Kasuga, Fukuoka 816-8580, Japan*
[3]*Institute of Observational Research for Global Change, Japan Agency for Marine-Earth Science and Technology, Yokosuka, Kanagawa 237-0061, Japan*
[4]*National Institute of Information and Communications Technology, Onna, Kunigami, Okinawa 904-0411, Japan*
[5]*Department of Electrical and Electronics Engineering, Faculty of Engineering, University of Ryukyus, Nishihara, Okinawa 903-0213, Japan*

(Received 18 October 2006; in revised form 7 February 2007; accepted 9 February 2007)

A method to extract geostrophic current in the daily mean HF radar data in the Kuroshio upstream region is established by comparison with geostrophic velocity determined from the along-track altimetry data. The estimated Ekman current in the HF velocity is 1.2% (1.5%) and 48° (38°)-clockwise rotated with respect to the daily mean wind in (outside) the Kuroshio. Furthermore, additional temporal smoothing is found necessary to remove residual ageostrophic currents such as the inertial oscillation. After removal of the ageostrophic components, the HF geostrophic velocity agrees well with that from the altimetry data with rms difference 0.14 (0.12) m/s in (outside) the Kuroshio.

Keywords:
· High-Frequency Ocean Radar,
· satellite altimetry,
· upstream of the Kuroshio,
· Ekman current,
· geostrophic velocity,
· inertial oscillation.

1. Introduction

Studies on variations of the ocean currents have progressed drastically thanks to the use of satellite altimetry. In the upstream region of the Kuroshio, for example, westward-propagating cyclonic (or anticyclonic) mesoscale eddies are found to merge with the Kuroshio east of Taiwan, subsequently inducing the decrease (or increase) of the surface volume transport in the Tokara Strait approximately 30 days later (Ichikawa, 2001). However, since maps of the sea surface height anomaly (SSHA) field are generally interpolated using along-track altimetry data for a period longer than 10 days (cycle of TOPEX/POSEIDON), such rapidly moving phenomena as meanders of the Kuroshio cannot be resolved well with these maps alone (Ichikawa *et al*., 1995). Moreover, temporal anomaly does not adequately describe variations of the Kuroshio having a strong mean component (Ichikawa and Imawaki, 1994).

Since July 2001, sea surface currents in the upstream region of the Kuroshio have been monitored by the high-frequency ocean radar (hereafter HF radar) system developed by the National Institute of Information and Communications Technology (NICT), Japan. HF radar measures the sea surface velocity component in the direction toward the radar, using the Doppler frequency shift of the radiowave backscattered by ocean surface wind waves within an observation cell (footprint) of the radar; the vector velocity is determined by combining observed radial velocity components of two (or more) radars (Sato *et al*., 2005). After comparison with vector velocity measured by a current meter at a fixed point, it was confirmed that the HF radar system developed by NICT measures surface velocity accurately (Matsuoka *et al*., 2003; Sato *et al*., 2004). Since the HF radar data have higher resolution in space and time than the satellite altimetry and they

* Corresponding author. E-mail: ichikawa@riam.kyushu-u.ac.jp

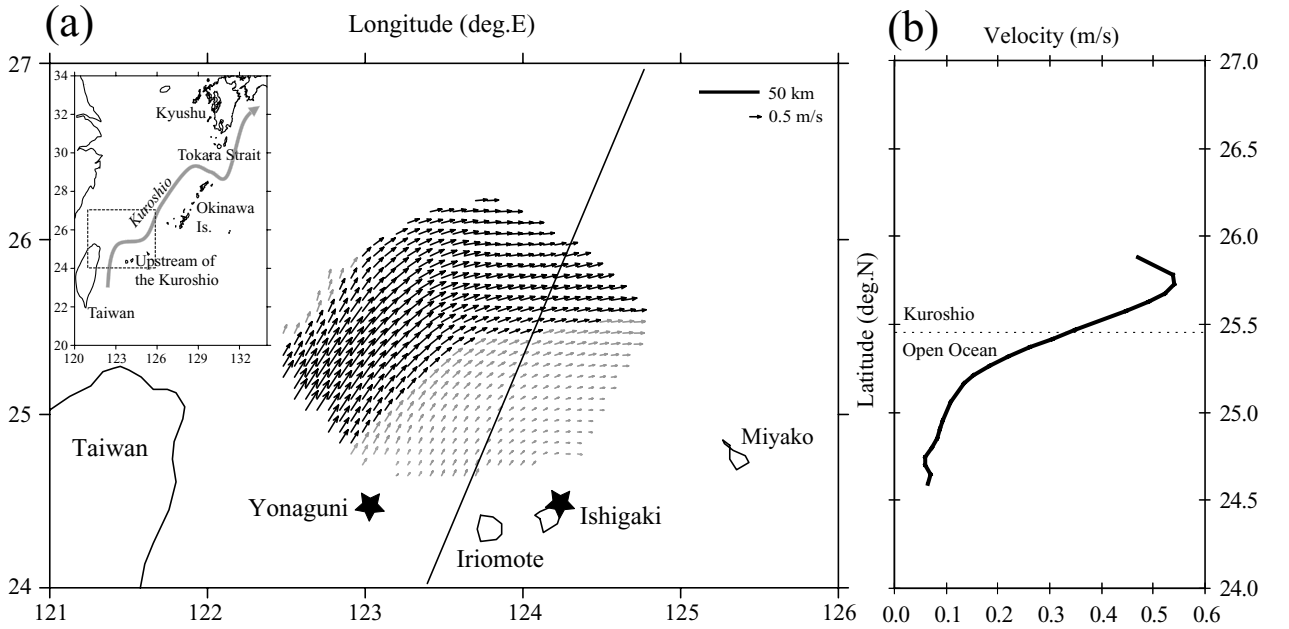

Fig. 1. 3.5-year mean HF vector velocity in the upstream of the Kuroshio (a); study area is indicated by a dashed square in a wider map of the Kuroshio at the top left corner. Black (or gray) vectors indicate the 3.5-year mean velocity of speed larger (smaller) than 0.5 m/s. Reference velocity of 0.5 m/s and scale of 50 km are plotted at the top right corner of the panel. Star marks show positions of the HF radars on Yonaguni and Ishigaki Islands. Oblique line indicates the subsatellite track used in this study. The velocity component normal to this subsatellite track is extracted along the track and plotted against the latitude (b); southeastward is defined as positive. Dotted line at 25.47°N indicates a boundary of the Kuroshio area where speed of the vector velocity in (a) exceeds 0.5 m/s.

are not confined to temporal anomaly, the HF radar system is considered more suitable to observe rapidly propagating disturbances of the Kuroshio in a limited observation area. Furthermore, combined use of the HF radar data with satellite altimetry or ship hydrographic data in a wider area could provide a more comprehensive description of variations of the Kuroshio due to its interaction with mesoscale eddies.

However, the sea surface velocity obtained with the HF radar (hereafter HF velocity) contains not only a geostrophic current component but also ageostrophic components, such as tidal, wind-driven Ekman currents and others. These ageostrophic currents are absent from the geostrophic data obtained with altimetry or hydrographic observations and make comparison difficult. The tidal component can be removed from time series of the HF velocity by harmonic analysis, but the Ekman component driven by local wind needs to be estimated using wind data. These estimates would be specific to HF observations since Ekman current depends strongly on the depth of measurements. In addition, the spatial and temporal characteristics of the estimated HF geostrophic velocity data need to be verified against independent data such as altimetry or hydrography.

The purpose of this study is therefore to develop a method for estimating the geostrophic velocity component of the HF velocity. We also discuss spatial and temporal scales of the estimated geostrophic velocity in the Kuroshio and in the open ocean, where dominant features have different scales. To achieve these goals, the HF velocity is compared with the reference geostrophic velocity, the velocity component normal to the subsatellite track calculated from the along-track altimetry data. This velocity component determined from the along-track altimetry data has been reported to agree with *in situ* surface velocity observations when it is spatially smoothed over the internal radius of deformation (Kashima *et al.*, 2003; Ito *et al.*, 2004). Note that the vector velocity calculated from the gridded SSHA field would not be adequate for the reference velocity due to smoothing in both space and time (Willebrand *et al.*, 1990; Ichikawa *et al.*, 1995, 2004; Yu *et al.*, 1995), although comparisons with vector HF velocity are possible throughout the study area. HF radar and altimeters data used in this study are described in Section 2, together with wind data used to estimate the wind-driven Ekman current component. HF velocity and the reference geostrophic velocity obtained from the altimetry data are first compared in Section 3,

and then a method to estimate the Ekman current component of the HF velocity is presented in Section 4. After removal of the Ekman current component, velocities of both the altimeter and HF radar are compared in Section 5, together with discussions.

2. Data

Each HF radar, placed on Ishigaki and Yonaguni Islands (Fig. 1(a)), measures the radial surface velocity component at 7-km and 0.5-hour intervals (Matsuoka *et al*., 2003; Sato *et al*., 2004). We use 3.5 years of gridded vector velocity data from July 2001 to January 2005, which are produced by NICT on a 7-km grid every 0.5 hours from those radial velocities (http://www2.nict.go.jp/y/y222/okinawa/EN/). In order to compare them with the geostrophic velocity calculated from the altimetry SSHA, we calculate the HF velocity anomaly as a deviation from the 3.5-year mean velocity (Fig. 1(a)); outlier data five standard deviations away from the mean were removed. In the mean velocity field (Fig. 1(a)), the Kuroshio is clearly recognized in the west, northwest and north of the study area as a band of strong northeastward velocity. In this paper we define the "Kuroshio area" as the area with mean velocity greater than 0.5 m/s, and the "open ocean area" is the rest of the domain.

In order to remove tidal components in the HF velocity, 11 tidal constituents (M2, S2, N2, K2, K1, O1, P1, Q1, Mf, Sa and Ssa) are first estimated by harmonic analysis at each grid point. Except for the non-astrometrical constituents Sa and Ssa, which are dominated by variations of ocean currents, the nine constituents that account for approximately 4.5% of the variance of the HF velocity were extracted (Yanagi *et al*., 1997). The one-day mean velocity is then calculated from the 0.5-hour velocity to reduce high-frequency variations; outliers over three standard deviations are excluded, and grid points are omitted if there are fewer than 24 samples in a day.

We use the SSHA data along the subsatellite track shown in Fig. 1(a), observed approximately every 10 days by TOPEX/POSEIDON and Jason-1 altimeters. The altimeter products were produced by SSALTO/DUACS and are distributed by AVISO with support from CNES (AVISO, 2004) as delayed-time data, in which corrections such as tides and air pressure have been applied with higher accuracy. The SSHA relative to the same 3.5-year mean is obtained at points along the subsatellite track with 7-km interval. The geostrophic velocity anomaly, v_{alt}, normal to the subsatellite track is calculated from the slope of the SSHA between adjacent points, which is defined as positive in the southeastward direction. Since the altimetry geostrophic velocity anomaly, v_{alt}, is known to agree well with *in situ* geostrophic velocity when it is smoothed over the internal radius of deformation (Kashima *et al*., 2003; Ito *et al*., 2004), the SSHA is spatially smoothed with a 42-km running mean along the subsatellite track in the Kuroshio area and with a 56-km one in the open ocean area (Emery *et al*., 1984; Chelton *et al*., 1998).

For comparison with the altimetry geostrophic velocity, v_{alt}, the gridded one-day mean HF velocity anomaly is interpolated onto the same points of the along-track SSHA data, and the HF velocity anomaly component, V_{hf}, normal to the subsatellite track is determined. Note that this HF velocity anomaly, V_{hf}, consists of the geostrophic current component, v_{hf}, and the ageostrophic current component, u; $V_{hf} = v_{hf} + u$. The geostrophic velocity, v_{hf}, observed with the HF radar could be different from the altimetry geostrophic velocity, v_{alt}, due to difference of the measurements (e.g. accuracy and spatiotemporal scales); hereafter, we denote the difference of two geostrophic velocities as "measurement difference", ε, namely $\varepsilon = v_{hf} - v_{alt}$. For convenience of further discussions, the 3.5-year mean velocity component normal to the subsatellite track similarly extracted at the same locations is shown in Fig. 1(b). In Fig. 1(b), the stronger flow of the Kuroshio is present to the north of 25.47°N.

The wind data for the estimation of the Ekman current component used in Section 4 is obtained from CERSAT, at IFREMER, Plouzané, France (CERSAT, 2002), which is daily mean vector wind on a 0.5-degree grid. The temporal wind anomaly, $\boldsymbol{W}$, relative to the mean of the same 3.5 years is then determined.

3. Comparison of HF Velocity V_{hf} with Altimetry Geostrophic Velocity v_{alt}

Along the subsatellite track, the temporal anomaly of the HF velocity, V_{hf}, normal to the track is first compared with the geostrophic velocity anomaly, v_{alt}, calculated from the altimetry data to examine the influence of the ageostrophic velocity component, u, of V_{hf} and the measurement difference, ε; for example, Fig. 2 shows profiles of V_{hf} and v_{alt} on 30 May 2003. In Fig. 2, both the one-day mean HF velocity anomaly, V_{hf} (solid line), and the geostrophic velocity anomaly, v_{alt}, calculated from the SSHA spatially smoothed over 56 km (dashed line) are found to be positive (or negative) to the north (or south) of 25.4°N. By combining with the 3.5-year mean velocity shown in Fig. 1(b), the northern positives in Fig. 2 indicate that the velocity component of the Kuroshio normal to the track reached 0.90 m/s around 25.7°N on that day. Meanwhile, the significant negatives in Fig. 2 correspond to a countercurrent south of 25.1°N with a northwestward component since the mean velocity there in Fig. 1(b) is less than the absolute value of the negative anomaly V_{hf} in Fig. 2.

Amplitudes of V_{hf} and v_{alt} variations are, however, different, especially in the open ocean area. In general, the amplitude of the v_{alt} variation depends on the spatial

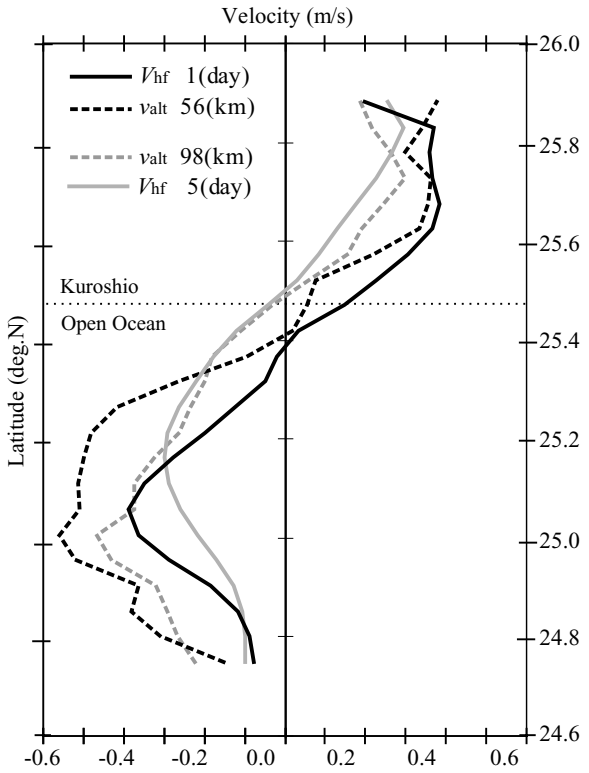

Fig. 2. One-day mean HF velocity anomaly component V_{hf} (solid line) and the geostrophic velocity anomaly component v_{alt} (dashed line) determined from the altimetry data with 56-km smoothing on 30 May, 2003. Temporally smoothed V_{hf} over five days (solid gray line) and spatially smoothed v_{alt} over 98 km (dashed gray line) are also plotted. Dotted line at 25.47°N indicates a boundary of the Kuroshio area and the open ocean area used in this paper.

smoothing scales (Ichikawa *et al.*, 2004). For example, if we smooth the SSHA over 98 km along the track (dashed gray line), the amplitude of the southern negative curve of the v_{alt} decreases by losing such small-scale structures as the sharp change at 25.3°N. It should also be noted that no spatial smoothing has been applied to V_{hf} in Fig. 2, suggesting the presence of either intrinsic spatial smoothing of the HF radar observations which causes the measurement difference, ε, or large-scale ageostrophic velocity component u.

Similarly, some ageostrophic currents u included in V_{hf}, with a small time scale, are expected to be reduced if we smooth V_{hf} in time, although some temporally-varying, quasi-geostrophic current v_{hf} may also be lost. If we average V_{hf}, for instance, over five days around 30 May 2003 (solid gray line), both positive and negative peaks at 25.7°N and 25.1°N appeared in the one-day mean V_{hf} are shifted northward to 25.8°N and 25.2°N. In this case, the five-day mean V_{hf} north of 25.2°N is rather similar to the 98-km smoothed geostrophic velocity, v_{alt}.

Such comparisons are made for many combinations of various temporal smoothing scales of V_{hf} and various spatial smoothing scales of v_{alt}. In these comparisons, the root-mean-square (rms) difference between V_{hf} and v_{alt} is calculated for all observation points along the subsatellite track during 3.5 years, both in the Kuroshio area and in the open ocean area (Fig. 3); the sampling number for the rms difference is about 800 in the Kuroshio area and about 1200 in the open ocean area. In Fig. 3, the rms difference between V_{hf} and v_{alt} tends to decrease with increasing spatial or temporal smoothing scales, resulting in the minimum that appears in the upper-right corner of each panel. In general, however, root sum of variances of V_{hf} and v_{alt} itself tends to be smaller with increasing spatial or temporal smoothing scales (Fig. 4). In order to remove this effect from the rms difference in Fig. 3 we define normalized difference as the rms difference divided by the corresponding root sum of variances of V_{hf} and v_{alt} shown in Fig. 4.

Unlike Fig. 3, the normalized difference in Fig. 5 does not change monotonously when increasing the spatial and temporal smoothing scales. In the Kuroshio area (Fig. 5(a)), an oblique area of smaller normalized difference exists from the lower-left side to the upper-right side. The normalized difference for a given temporal smoothing scale of V_{hf} first decreases as the spatial smoothing scale of v_{alt} increases, but then starts to increase after the spatial smoothing scale exceeds a certain scale. Since the normalized difference would increase when v_{alt} is over-smoothed or under-smoothed with respect to the spatial scale of the given V_{hf}, the spatial smoothing scale of v_{alt} that results in the smallest normalized difference is considered to indicate the spatial scale of the given V_{hf} itself.

Similarly, the normalized difference for a given spatial smoothing scale of v_{alt} shows both a first decrease and a subsequent increase as the temporal smoothing scale of V_{hf} increases. Since the Kuroshio is known to have great temporal variability, the increase would be induced by the measurement difference, ε, as a loss of the temporally-varying, quasi-geostrophic current component v_{hf} due to over-smoothing of V_{hf} in time. Analogously, the decrease would be caused by temporal under-smoothing of V_{hf}. In this case, the under-smoothing may be originated by two causes respectively related to ε and u; the smoothing scale of V_{hf} in time is either shorter than the temporal scale of the given v_{alt}, or too short to average out some short-term ageostrophic currents of u in V_{hf}.

The latter cause would be obviously recognized in the open ocean area (Fig. 5(b)). For the one-day mean V_{hf} in Fig. 5(b), the normalized difference is especially larger than any other temporal smoothing scales, whatever the spatial smoothing scale of v_{alt} is. This suggests that some short-term ageostrophic currents u such as inertial oscil-

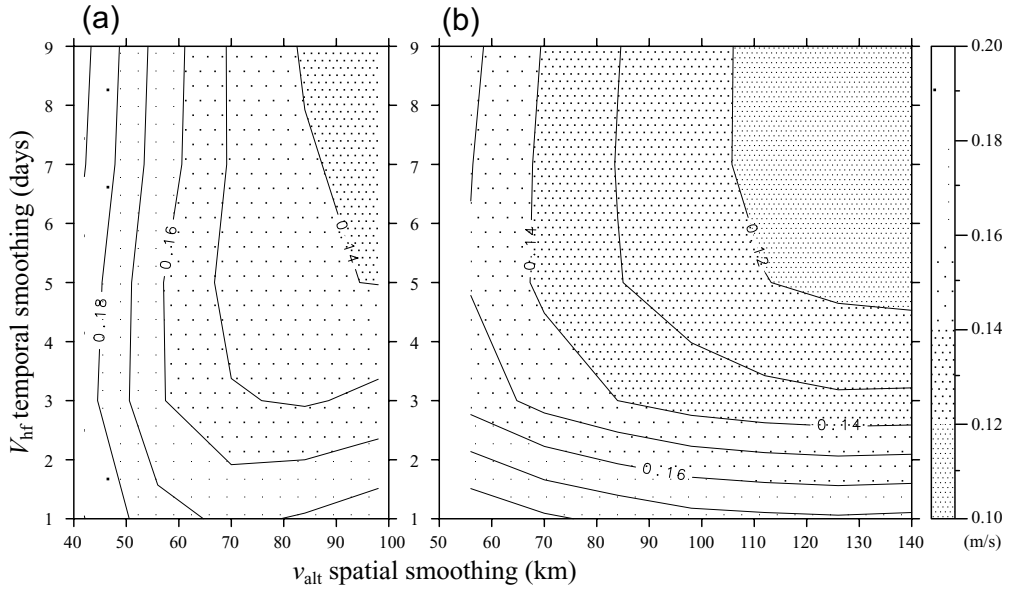

Fig. 3. Rms difference between HF velocity V_{hf} and geostrophic velocity v_{alt} in the Kuroshio area (a) and in the open ocean area (b). Geostrophic velocity v_{alt} is smoothed over various (42, 56, 70, 84, 98, 112, 126 and 140 km) spatial scales along the subsatellite track (horizontal axis), while HF velocity V_{hf} is averaged over various (1, 3, 5, 7 and 9 days) temporal scales (vertical axis). Contour and shading intervals are 0.01 and 0.02 m/s, respectively, accounting for significant differences of χ^2-test at 95% confidence level in the open ocean and Kuroshio areas, respectively.

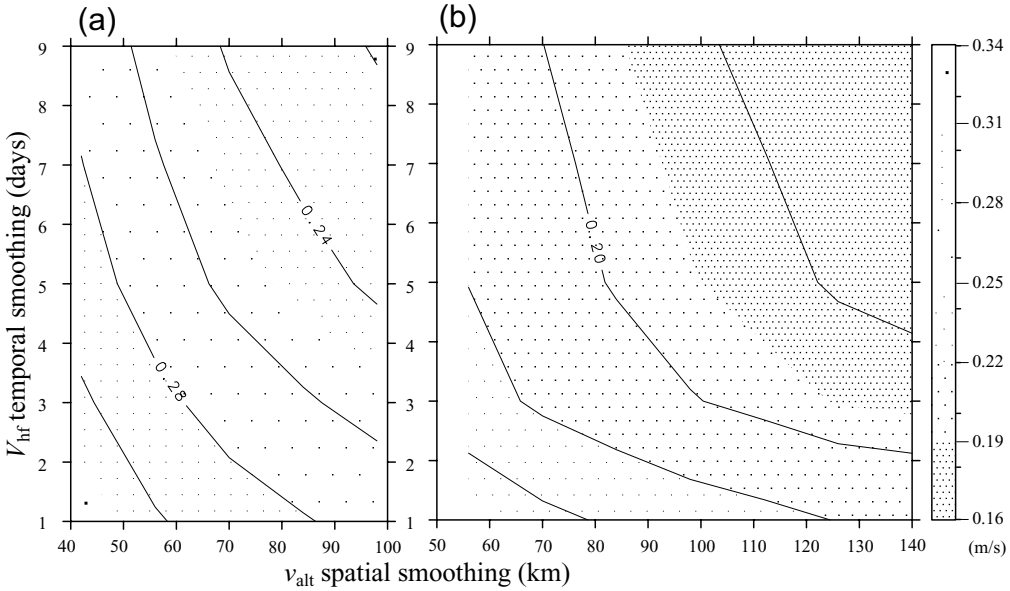

Fig. 4. Root sum of variances of the HF velocity V_{hf} and the geostrophic velocity v_{alt} in the Kuroshio area (a) and in the open ocean area (b). Axes, contour and shading intervals are as Fig. 3, except for values of the intervals (0.02 and 0.03 m/s, respectively).

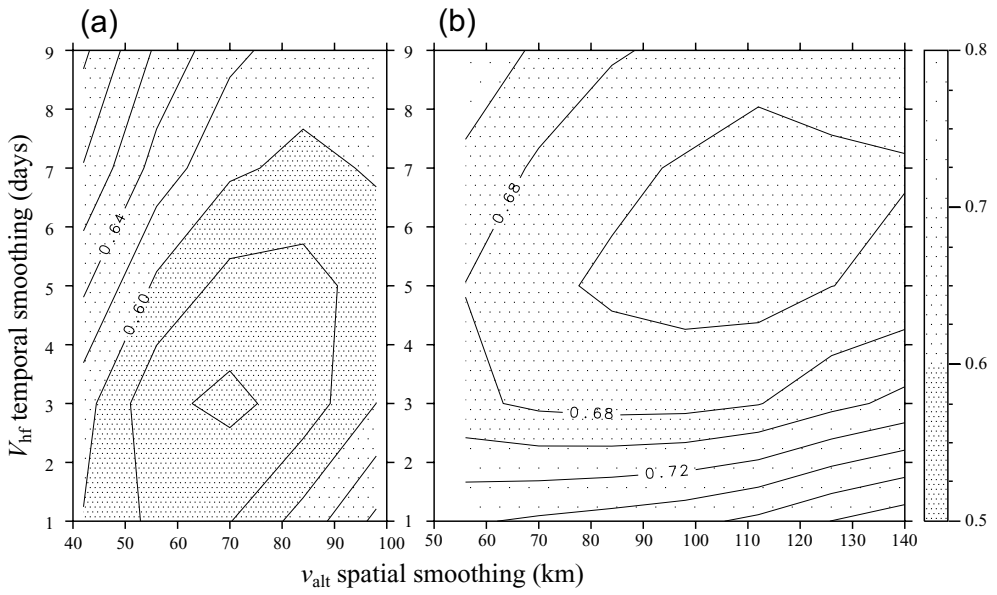

Fig. 5. As Fig. 3 but showing normalized difference. Shading interval is 0.1, accounting for significant differences shown in Figs. 3 and 4. Contour interval is set to 0.02 for convenience.

lation and Ekman current driven by short-term wind variation remain in the one-day mean V_{hf}. Note that these ageostrophic currents u would be less significant compared to the strong geostrophic current in the Kuroshio area, so that they would result in smaller values if normalized by the root sum of variances shown in Fig. 4. Actually, the rms differences for the one-day mean V_{hf} are nearly the same (approximately 0.17 m/s) in both areas (Figs. 3(a) and (b)).

For temporal smoothing scales longer than three days, the normalized difference represents the sum of the measurement difference, ε, and such longer-term ageostrophic currents u as the Ekman current induced by winds with temporal scales longer than three days. The decrease of the normalized difference there in the open ocean area becomes as gradual as the increase, which would suggest that these changes are mainly produced by variation of the measurement difference, ε, due to temporal smoothing of v_{hf}. An oblique area of smaller normalized difference also exists in Fig. 5(b), as seen in the Kuroshio area (Fig. 5(a)); the presence of the oblique area of smaller ε is reasonable since the spatial scale of geostrophic currents generally tends to be larger when the temporal scale increases. The width of the oblique area in the Kuroshio area, however, is noticeably narrower than that in the open ocean area. This would be caused by difference of sensitivity to over-smoothing or under-smoothing of v_{alt} in each area. In the Kuroshio area, where distinct velocity structures with relatively small spatial scales exist, a large difference in ε would be produced if the velocity field, v_{alt}, is over-smoothed or under-smoothed compared to the given spatial scale of v_{hf}.

The minimum normalized difference in the Kuroshio area (or the open ocean area) occurs when v_{alt} is smoothed over 70 km (or 112 km) and V_{hf} is smoothed over three (or five) days, although these minimum values are not significantly different from the surroundings in Fig. 5.

4. Estimating Wind-Driven Ekman Current u_w in the HF Velocity V_{hf}

The wind-driven Ekman current would not be averaged out by temporal smoothing since the forcing winds include a longer time-scale variation component. Therefore, we estimate the Ekman component in the HF velocity as the ageostrophic component, u, that linearly corresponds to the wind vector, $\boldsymbol{W}$; hereafter, we distinguish the Ekman current component, u_w, from the other ageostrophic currents, u_o; namely, $u = u_w + u_o$.

The one-day mean Ekman current component normal to the subsatellite track, u_w, is expressed by using the one-day mean wind vector, $\boldsymbol{W} = [W_n, W_p]$ as:

$$u_w = \alpha \cdot W_n \cdot \cos\theta - \alpha \cdot W_p \cdot \sin\theta,$$

where W_n and W_p are the wind components normal and parallel to the subsatellite track, respectively, and α and θ are the unknown speed factor and rotation angle of the Ekman current with respect to the wind vector, respectively. Note that both wind vector, $\boldsymbol{W}$, and estimated u_w are defined as the anomaly from the 3.5-year mean, the

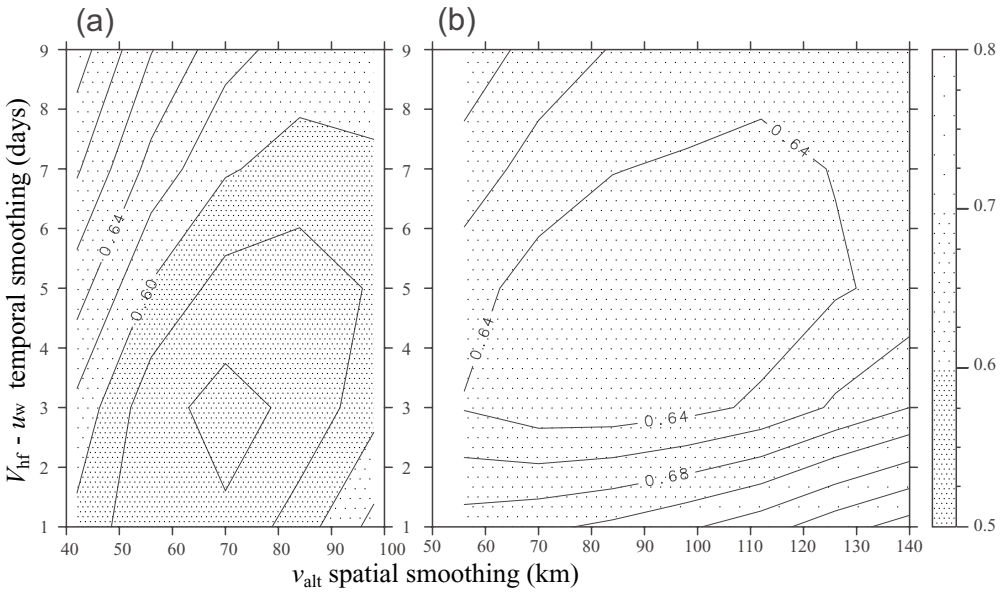

Fig. 6. As Fig. 5 but with the Ekman current component (u_w) removed from the HF velocity, V_{hf}.

same as V_{hf} and v_{alt}. These unknown parameters are to be determined by the least squares method, which minimizes the sum of squared differences between u_w and the ageostrophic currents, u, in the one-day mean V_{hf}; i.e., $\sum(u - u_w)^2$. The ageostrophic component, u, is defined as the one-day mean V_{hf} minus the geostrophic velocity, v_{hf}, observed with the HF radar. The latter v_{hf} would be equivalent to the altimetry geostrophic velocity, v_{alt}, that is smoothed properly in space so as to make the measurement difference, ε, negligible, but the spatial scale of v_{hf} itself is not well understood. Therefore we use v_{alt} with various spatial smoothing scales to calculate $S = \sum(V_{hf} - v_{alt} - u_w)^2$, then best fit parameters of α and θ are estimated independently in each area.

Estimated parameters α and θ that minimize S for each smoothing scale of v_{alt} are applied to the one-day mean wind vector, $\boldsymbol{W}$, in each area, and estimated Ekman current component, u_w, is extracted from the one-day mean V_{hf} to produce $(V_{hf} - u_w) = (v_{hf} + u_o)$. In the Kuroshio area, the normalized difference between the estimated one-day mean $(v_{hf} + u_o)$ and v_{alt} becomes smallest when the 56-km smoothed v_{alt} is used; for this case, the estimated speed factor, α, and rotation angle, θ, of the Ekman current, u_w, are 1.2% and 48° clockwise with respect to the one-day mean wind vector. Meanwhile, in the open ocean area, the smallest difference occurs when the 56-km smoothed v_{alt} is used; the parameters are 1.5% and 38°.

Estimations of the Ekman current from wind vector have been reported in previous studies. For example, using 6-hour-interval HF velocity data during the passage of a typhoon, Matsuoka *et al*. (2003) estimated that the wind speed factor ranges from 3.4 to 4.2% and the rotation angle from 35° to 39°. Meanwhile, the parameters estimated from altimetry geostrophic velocity and two-day averaged surface drifter data correspond to 0.8% and 54° at 25°N (Cornuelle *et al*., 2002; Niiler *et al*., 2003). The parameters obtained in this study for the one-day mean Ekman current is consistently situated between these two estimates. Quantitative comparisons are difficult, though, because the corresponding depths of these estimates are different; the Ekman current for drifter data is at about 15 m depth where drogues of drifters are located, whereas the depth represented in the HF velocity is considered to be about 1.3 m for this HF radar system (Matsuoka *et al*., 2003). More detailed studies would be necessary for further discussion, taking account of the vertical structure of the Ekman current (e.g. Wu, 1980; Donelan *et al*., 1993; Craig and Banner, 1994; Craig, 1996; Teague *et al*., 2001; Yoshikawa *et al*., 2007).

5. Summary and Discussions of the HF Geostrophic Velocity v_{hf}

Using the best-fit parameters for u_w estimated in the previous section, normalized differences between $(V_{hf} - u_w)$ and v_{alt} are determined for many combinations of various temporal smoothing scales of the former and various spatial smoothing scales of the latter (Fig. 6). Not only for the one-day mean $(V_{hf} - u_w)$ but also for the temporally longer smoothed $(V_{hf} - u_w)$, all values become smaller than corresponding ones in Fig. 5. Such reductions would be induced by removal of u_w caused by wind

variations with longer periods, such as seasonal wind variations. The improvement is especially noticable in the open ocean area where the Ekman current is less negligible with respect to the geostrophic velocity.

However, in the open ocean area, the extremely large normalized difference for the one-day mean ($V_{hf} - u_w$) still remains, even after removal of u_w. This tendency is also confirmed, even if we spatially smooth the gridded one-day mean vector HF velocity before ($V_{hf} - u_w$) is extracted along the subsatellite track, suggesting that the cause of the difference in the one-day mean ($V_{hf} - u_w$) has a large spatial scale. One possible reason for this residual difference is that the simple assumption is not adequate to estimate the daily Ekman current, u_w, linearly from the daily wind vector alone; a more complicated formula might be necessary, although the accuracy of the data used in the present paper would limit further extension. A more probable explanation is that the other ageostrophic component, u_o, remains in the one-day mean ($V_{hf} - u_w$), the temporal scale of which is longer than one day but shorter than three days. Since the inertial period at this latitude is 28 hours, the inertial oscillation, which has a large spatial scale, would not be averaged out in the 24-hour mean. It is therefore concluded that the daily mean Ekman-corrected HF velocity, ($V_{hf} - u_w$), should be further smoothed in time to obtain HF geostrophic velocity, v_{hf}, by excluding the residual ageostrophic components, u_o, such as the inertial oscillation, especially in the open ocean area where v_{hf} is not sufficiently large to neglect u_o.

The minimum normalized difference in Fig. 6 is for the 70-km smoothed v_{alt} and the three-day mean ($V_{hf} - u_w$) in the Kuroshio area, and for the 98-km smoothed v_{alt} and the five-day mean ($V_{hf} - u_w$) in the open ocean area. Although the minimum values are not significantly different from the surroundings, it should be noted that the spatial smoothing scale of v_{alt} for the minimum normalized difference in the open ocean area decreases after removal of u_w (Figs. 5(b) and 6(b)). This would be consistent, since the Ekman current, u_w, in V_{hf} is considered to have a larger atmospheric horizontal scale.

Figure 7 shows scatter diagrams for the altimetry geostrophic velocity, v_{alt}, versus the HF velocity, ($V_{hf} - u_w$) = ($v_{hf} + u_o$), for those minimum normalized differences. The minimum normalized difference corresponds to the rms difference of 0.14 m/s in the Kuroshio area and 0.12 m/s in the open ocean area. Assuming that the ageostrophic currents component, u_o, is negligible in these cases, these rms differences are considered to be induced by the measurement difference, $\varepsilon = v_{hf} - v_{alt}$. Since the spatial and temporal scales of v_{hf} and v_{alt} are regarded as fitting each other for these cases, the measurement difference, ε, would be mainly derived from the accuracy of observations of the HF velocity, v_{hf}, and the altimetry geostrophic velocity, v_{alt}. For the HF velocity, accuracy of a single measurement is estimated to be 0.15 m/s by

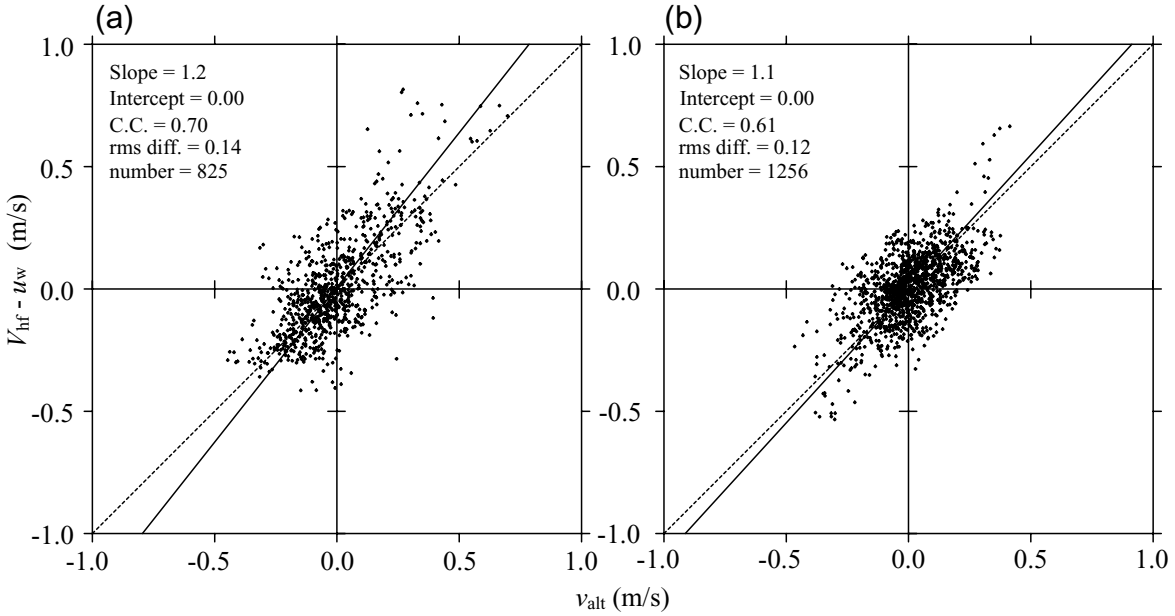

Fig. 7. Scatter plot of the 70-km smoothed v_{alt} versus the three-day smoothed ($V_{hf} - u_w$), producing the minimum normalized difference in the Kuroshio area (a), and that for the 98-km smoothed v_{alt} versus the five-day smoothed ($V_{hf} - u_w$) in the open ocean area (b). Linear regression is shown by solid lines, where dashed lines indicate ($V_{hf} - u_w$) = v_{alt}. Slope and intercept of the linear regression, correlation coefficient, rms difference and the number of data used are also shown in each panel.

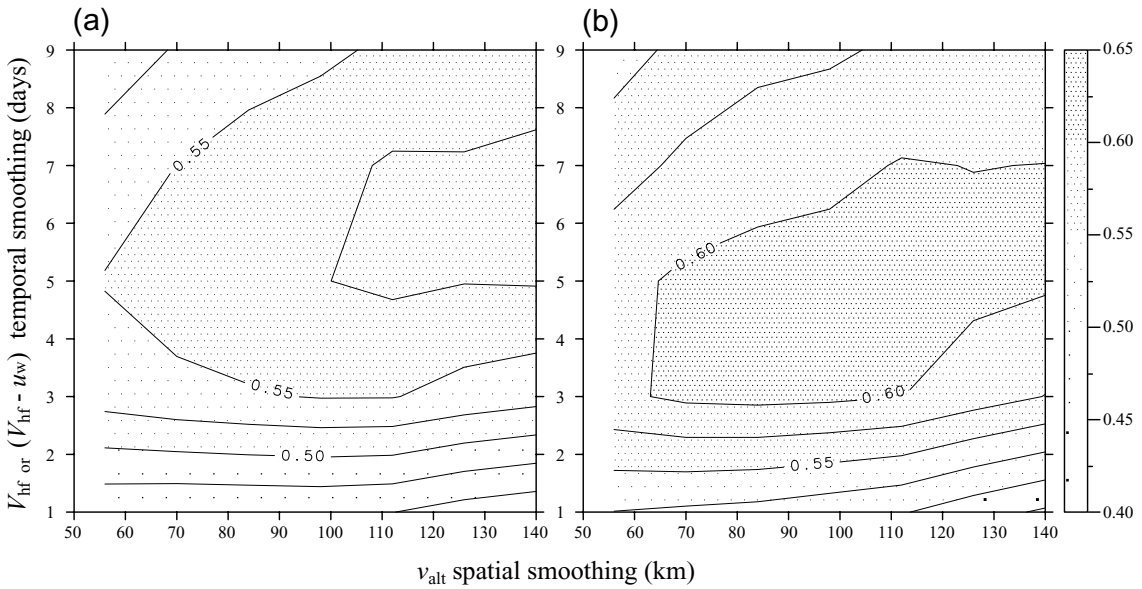

Fig. 8. Correlation coefficient in the open ocean area between the geostrophic velocity v_{alt} and the HF velocity V_{hf} before removal of the Ekman current (a), and ($V_{hf} - u_w$) after the removal (b). Horizontal and vertical axes are as Fig. 3(b). Shading interval is 0.05, accounting for significant difference by Fisher's z-test at 95% confidence level (Press *et al*., 1992). Contour interval is set as one-half of the shading interval.

comparison with *in situ* surface velocity observations at a moored buoy (Sato *et al*., 2004), although this could be overestimated for the temporally-smoothed velocity. For the geostrophic velocity determined from the along-track altimetry data, the accuracy has been reported to be 0.16 m/s in the Kuroshio south of Shikoku (Uchida *et al*., 1998) and 9.1×10^{-2} m/s in the open ocean (Ito *et al*., 2004). This suggests that the estimated HF geostrophic velocity, v_{hf}, would have at least similar accuracy to that of the altimetry geostrophic velocity, v_{alt}.

It is not only in the normalized difference shown in Figs. 5 and 6 that the improvement after removal of the Ekman current, u_w, is confirmed, but also in the correlation coefficient increases (Fig. 8). In addition, it should be noted that the distribution patterns of the correlation coefficient shown in Fig. 8(a) are much closer to that of the normalized difference (Fig. 5(b)) than that of the rms difference (Fig. 3(b)), which reasonably supports the use of the normalized difference instead of the rms difference. Both in the Kuroshio (figures not shown) and open ocean areas, the spatial and temporal smoothing scales for the maximum correlation are confirmed to agree with those for the minimum normalized difference, except for the case comparing V_{hf} and v_{alt} in the open ocean area (Figs. 5(b) and 8(a)). The maximum correlation in Fig. 8(a) occurs when v_{alt} is smoothed over 140 km and V_{hf} is averaged over seven days, but the maximum value is not significantly different from the surroundings. Actually, when the slope of the linear regression between v_{alt} and V_{hf} is accounted for, together with Fig. 8(a), the smoothing scales for the best comparison produce the same result as those for the minimum normalized difference in Fig. 5(b).

In this study we have demonstrated that the HF geostrophic velocity v_{hf} would be obtained with at least similar accuracy to the geostrophic velocity, v_{alt}, determined by satellite altimetry. Although the comparisons in this paper are limited to the subsatellite track and the component normal to it, the HF radar system can provide a mapped vector velocity within the radar range. By using the mapped HF geostrophic velocity after proper correction for ageostrophic currents described in this paper, rapidly moving phenomena such as the interaction between the Kuroshio and mesoscale eddies are remarkably well described, which will be reported in another paper (Ichikawa *et al*., 2007).

Acknowledgements

The authors would like to thank Professor Shiro Imawaki for his invaluable comments. Discussions with Dr. Shinichiro Umatani and Dr. Yutaka Yoshikawa were especially useful in interpreting the results. The authors also appreciate helpful suggestions from anonymous reviewers. This work is part of a project called "Monitoring and prediction of marine and atmospheric environmental changes in the East Asia" of the Research Insti-

tute for Applied Mechanics, Kyushu University. This paper is also partially sponsored by Hydrospheric Atmospheric Research Center, Nagoya University, as a part of collaborative research programs.

References

AVISO (2004): Ssalto/Duacs User Handbook: (M)SLA and (M)ADT Near-Real Time and Delayed Time Products. SALP-MU-P-EA-21065-CLS, Edition 1.2.

CERSAT (2002): QUIKSCAT SCATTEROMETER MEAN WIND FIELD PRODUCTS USER MANUAL. C2-MUT-W-03-IF, Ver. 1.0.

Chelton, D. B., A. D. Roland, G. S. Michael, E. N. Karim and S. Nicolas (1998): Geographical variability of the first baroclinic Rossby radius of deformation. *J. Phys. Oceanogr.*, **28**, 433–460.

Cornuelle, B. D., B. Beckley, P. P. Niiler, C. J. Koblinsky and N. Barth (2002): A statistical model for time-varying, wind-driven currents based on altimeter and Pacific drifter data. *Eos Trans. AGU*, **83**(4), Ocean Sci. Meet. Suppl., abstract OS32G-226.

Craig, P. D. (1996): Velocity profiles and surface roughness under breaking waves. *J. Geophys. Res.*, **101**(C1), 1265–1277.

Craig, P. D. and M. L. Banner (1994): Modeling wave-enhanced turbulence in the ocean surface layer. *J. Phys. Oceanogr.*, **24**, 2546–2559.

Donelan, M. A., F. W. Dobson, S. D. Smith and R. J. Anderson (1993): On the dependence of sea surface roughness on wave development. *J. Phys. Oceanogr.*, **23**, 2143–2149.

Emery, W. J., W. G. Lee and L. Magaard (1984): Geographic and seasonal distributions of Brunt-Väisälä frequency and Rossby Radii in the North Pacific and North Atlantic. *J. Phys. Oceanogr.*, **14**, 294–317.

Ichikawa, K. (2001): Variation of the Kuroshio in the Tokara Strait induced by meso-scale eddies. *J. Oceanogr.*, **57**, 55–68.

Ichikawa, K. and S. Imawaki (1994): Life history of a cyclonic ring detached from the Kuroshio Extension as seen by the Geosat altimeter. *J. Geophys. Res.*, **99**(C8), 15953–15966.

Ichikawa, K., S. Imawaki and H. Ishii (1995): Comparison of surface velocities determined from altimeter and drifting buoy data. *J. Oceanogr.*, **51**, 729–740.

Ichikawa, K., N. Gohda, M. Arai and A. Kaneko (2004): Monitoring surface velocity from repeated ADCP observations and satellite altimetry. *J. Oceanogr.*, **60**, 365–374.

Ichikawa, K., R. Tokeshi, M. Kashima, K. Sato, T. Matsuoka, S. Kojima and S. Fujii (2007): Kuroshio variations in the upstream region as seen by HF radar and satellite altimegry data. *Intr. J. Remote Sensing* (submitted).

Ito, S., K. Uehara, T. Miyao, H. Miyake, I. Yasuda, T. Watanabe and Y. Shimizu (2004): Characteristics of SSH anomaly based on TOPEX/POSEIDON altimetry and *in situ* measured velocity and transport of Oyashio on OICE. *J. Oceanogr.*, **60**, 425–437.

Kashima, M., S. Imawaki, S. Umatani, H. Uchida, Y. Hashibe, H. Ichikawa and M. Fukasawa (2003): Geostrophy in the intermediate and deep layers of the Kuroshio and its recirculation regions south of Japan. *J. Oceanogr.*, **59**, 291–301.

Matsuoka, T., K. Sato, S. Kojima and S. Fujii (2003): HF ocean radar observation of surface currents induced by a typhoon in the East China Sea. *IEEE Proceedings of International Geoscience and Remote Sensing Symposium 2003*, No.I-F05-03.

Niiler, P. P., N. A. Maximenko, G. G. Panteleev, T. Yamagata and D. B. Olson (2003): Near-surface dynamical structure of the Kuroshio Extension. *J. Geophys. Res.*, **108**(C6), 3193, doi:10.1029/2002JC001461.

Press, W. H., S. A. Teukolsky, W. T. Vetterling and B. P. Flannery (1992): *Numerical Recipes in FORTRAN; The Art of Scientific Computing*. 2nd ed., Cambridge Univ. Press, 963 pp., ISBN 0-521-43064-X.

Sato, K., T. Matsuoka, S. Kojima and S. Fujii (2004): Long-range ocean radar observation of Kuroshio upstream region in the East China Sea. *Bull. Coast. Oceanogr.*, **41**, 119–127 (in Japanese with English abstract).

Sato, K., S. Kojima and T. Matsuoka (2005): Accuracy evaluation of surface current velocity measured by Bistatic HF Ocean Radar. *IEICE Technical Report SANE2005-87* (in Japanese with English abstract).

Teague, C. C., J. F. Vesecky and Z. R. Hallock (2001): A comparison of multifrequency HF radar and ADCP measurements of near-surface currents during COPE-3. *J. Oceanic Engin.*, **26**(3), 399–405.

Uchida, H., S. Imawaki and J. Hu (1998): Comparison of Kuroshio surface velocities derived from satellite altimeter and drifting buoy data. *J. Oceanogr.*, **54**, 115–122.

Willebrand, J., R. H. Kase, D. Stammer, H.-H. Hinrichsen and W. Krauss (1990): Verification of Geosat sea surface topography in the Gulf Stream Extension with surface drifting buoys and hydrographic measurements. *J. Geophys. Res.*, **95**(C3), 3007–3014.

Wu, J. (1980): Wind stress coefficients over the sea surface near neutral conditions—A revisit. *J. Phys. Oceanogr.*, **10**, 727–740.

Yanagi, T., A. Morimoto and K. Ichikawa (1997): Co-tidal and co-range charts for the East China Sea and the Yellow Sea derived from satellite altimetric data. *J. Oceanogr.*, **53**, 303–309.

Yoshikawa, Y., T. Matsuno, K. Marubayashi and K. Fukudome (2007): A surface velocity spiral observed with ADCP and HF radar in the Tsushima Strait. *J. Geophys. Res.* (accepted).

Yu, Y., W. J. Emery and R. R. Leben (1995): Satellite altimeter derived geostrophic currents in the western tropical Pacific during 1992–1993 and their validation with drifting buoy trajectories. *J. Geophys. Res.*, **100**(C12), 25,069–25,085.